

# A numerical model for heat and pressure propagation for temperature controlled retinal photocoagulation

Alexander Baade\*<sup>a</sup>, Kerstin Schlott<sup>a</sup>, Reginald Birngruber<sup>a,b</sup>, Ralf Brinkmann<sup>a,b</sup>

<sup>a</sup>Medizinisches Laserzentrum Lübeck GmbH, Peter-Monnik-Weg 4, 23562 Lübeck, Germany;

<sup>b</sup>Institut für Biomedizinische Optik, Universität zu Lübeck, Peter-Monnik-Weg 4, 23562 Lübeck, Germany

## ABSTRACT

Retinal photocoagulation is an established treatment for various retinal diseases. The temperature development during a treatment can be monitored by applying short laser pulses in addition to the treatment laser light. The laser pulses induce thermoelastic pressure waves that can be detected at the cornea. We present a numerical model to examine the temperature development during the treatment as well as the formation and propagation of the ultrasonic waves. Using the model, it is possible to determine the peak temperature during retinal photocoagulation from the measured signal, and investigate the behaviour of the temperature profile and the accuracy of the temperature determination under varying conditions such as inhomogeneous pigmentation or change in irradiation parameters. It was shown that there is an uncertainty of 2.5 -9% in the determination of the peak temperature when the absorption coefficient between the absorbing layers is varied by a factor of 2.

Furthermore the model was extended in order to incorporate the photoacoustic pressure generation and wave propagation. It was shown that for an irradiation pulse duration of 75 ns the resulting pressure wave energy is attenuated by 76 % due to frequency dependent attenuation in water.

**Keywords:** Optoacoustics, Ophthalmology, Light-Tissue-Interaction, Numerical temperature Modeling, Numerical pressure Modeling, COMSOL

## 1. INTRODUCTION

Photocoagulation is a widely used treatment method for retinal diseases such as diabetic retinopathy and macula edema<sup>1-3</sup>. During the treatment laser light is applied onto the fundus. Using a wavelength in the green spectral band, the radiation is absorbed mainly in the retinal pigment epithelium (RPE), a strongly pigmented cellular monolayer located between the neural retina and the choroid. The deposited energy causes an increase in temperature which leads to a therapeutically desired coagulation of the fundus tissue after exceeding the damage threshold temperature.

However, intra- and interocularly varying pigmentation of the RPE and choroid, as well as light scattering within the anterior parts of the eye makes it difficult for the physician to choose the correct laser parameters to avoid under- or overtreatment, which in the worst case can lead to rupture and bleeding at the retina. Therefore, a real-time temperature measurement is desirable in order to select the appropriate laser parameters automatically.

Optoacoustics is a method to excite ultrasonic waves by pulsed laser irradiation. Over the past years, it has become a modality in diagnostics<sup>4</sup> and imaging<sup>5</sup>. Also, it has been shown that this method can be used to measure temperatures in real-time<sup>6,7</sup>. It is also suitable to monitor the temperature development in the eye during transpupillary thermo therapy (TTT)<sup>7</sup> and laser photocoagulation<sup>8</sup>.

This work examines the accuracy of real-time temperature determination during laser photocoagulation of the retina using a numerical model for heat diffusion, thermal expansion and pressure propagation.

## 2. MATERIALS AND METHODS

There are two main challenges when determining the peak temperature at the center of the RPE from the measured pressure amplitude, the highest temperature where tissue denaturation is expected to set in first. First of all, the pressure rise is dependent on several tissue parameters, for example the degree of pigmentation and the thermal expansion coefficient. However, these parameters are different for each individual location, so the temperature dependency of the pressure is usually unknown prior to the treatment. A calibration measurement for retinal tissue was conducted in order to calculate the temperature from the pressure rise<sup>8</sup>.

Secondly, the temperature distribution is not spatially and axially homogeneous and its profile also varies with time. However, all absorbers irradiated by the probe beam contribute to the photoacoustic response according to their respective base temperature. The resulting pressure wave contains temperature information from all these volume elements, so the resulting piezoelectric signal from the ultrasonic transducer represents a mean photoacoustic response and therefore the measured pressure value will give a mean temperature of the irradiated tissue volume. The peak temperature can be determined from the measured mean temperature by considering the temperature evolution using a theoretical eye model.

### 2.1 Optoacoustic Pressure Generation

If a laser pulse is applied to an absorber, the temperature of the absorber rises by  $\Delta T$ , leading to a thermoelastic expansion and the subsequent emission of a pressure wave. Under the condition of thermal and stress confinement the generated local pressure increase  $\Delta P(r,t)$  is proportional to the temperature increase  $\Delta T$  caused by the pulsed laser light and the Grüneisen parameter  $\Gamma(T)$ <sup>7</sup>:

$$\Delta P(r,t) \propto \Gamma(T)\Delta T(r,t) . \quad (1)$$

Due to the temperature dependency of the Grüneisen parameter  $\Gamma(T)$ , the resulting pressure wave amplitude  $p(T)$  is also temperature dependent and can be approximated with a second order polynomial<sup>7</sup>:

$$p(T) = sE[(T^2 - T_0^2) - 2T_{\max}(T - T_0)], \quad (2)$$

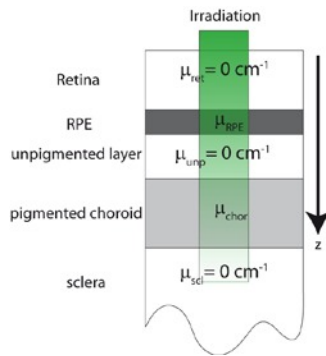
where  $E$  is the laser pulse energy and  $s$  is a proportionality constant that depends on signal and detector characteristics as well as the light and sound transmission through the eye and the pigmentation at each irradiated spot.  $T_0$  and  $T_{\max}$  are tissue specific parameters that have to be determined by a calibration measurement<sup>8</sup>.

For a uniform temperature of the absorber the optoacoustically determined temperature  $T_{\text{OA}}$  corresponds to the tissue temperature and can be determined from the measured pressure  $p(T)$  by solving eq. 2 for  $T$

$$T_{\text{OA}}(p) = T_{\max} - \sqrt{T_{\max}^2 + \frac{p}{sE} + T_0^2 - 2T_{\max}T_0} . \quad (3)$$

### 2.2 Temperature and Heat Diffusion Equation

Figure 1 shows the used fundus layer model for a human eye along with the respective tissue layer absorption coefficients  $\mu_a$  and layer thicknesses  $d$ . The irradiation passes the retina, where only about 3-5% of the light is absorbed and will be neglected here. About half of the irradiation is absorbed in the RPE, and then passes the unpigmented part of the choroid. The rest of the light is absorbed in the pigmented part of the choroid.



	$\mu_a$ [cm <sup>-1</sup> ]	$d$ [μm]
Retina	0	N.A.
RPE	1204	6
unpigm. choroid	0	4
pigm. choroid	270	300

Figure 1 Fundus model for a human eye with layer absorption coefficients  $\mu_a$  and thickness  $d$ .

The radial ( $r$ ) and axial ( $z$ ) temperature distribution at the fundus during retinal photocoagulation can be obtained by solving the heat diffusion equation:

$$\rho C_p \frac{\partial T(\vec{r}, t)}{\partial t} - \nabla \cdot (k \cdot \nabla T(\vec{r}, t)) = Q, \quad (4)$$

where  $\rho$  is the material density,  $\kappa$  the thermal conductivity,  $C_p$  the heat capacity and  $Q$  a heat source. The solution to eq. 4 is discussed elsewhere<sup>7</sup>.

When heating the fundus, the radiation is absorbed in the RPE and the pigmented choroid according to the model. Due to heat diffusion, the temperature in the surrounding media will also increase. Similarly, when probing with a short laser pulse, the optoacoustic pressure waves will be excited in the RPE and choroid, according to the base temperature and remaining light intensity at each absorber. As the temperature profile varies radially and axially, each absorbing volume element gives rise to a specific pressure wave, the waves will superimpose and travel through the tissue. Hence, this resulting pressure wave corresponds to a mean temperature of the irradiated volume. Using the fundus model as shown in fig. 2, the mean weighted temperature  $T_{\text{mean}}$ , which can be measured using optoacoustics is given for any time  $t$  by

$$T_{\text{mean}}(t) = \int_0^{z_0} T_{\text{av}}(z, t) \cdot w(z) \cdot dz, \quad (5)$$

where  $w(z)$  is the weight factor for the depth  $z$  given by  $w(z) = \mu_a(z) \cdot I(z) / I_0$ ,  $I(z)$  is the irradiance in the depth  $z$ , and  $z_0$  is the maximum penetration depth. Since the intensity of the probe beam drops exponentially with tissue depth  $z$  from  $I_0$  to  $I(z)$ , the optoacoustic response of the tissue also drops exponentially, according to Lambert-Beer's law which is considered by the weight function  $w(z)$ .  $T_{\text{av}}(z, \tau)$  is the average temperature over a cross section in a certain depth  $z$ ,

$$T_{\text{av}}(z, t) = \frac{2}{R^2} \int_0^R r \cdot T(r, z, \tau) \cdot dr. \quad (6)$$

However, the mean weighted temperature is not a suitable parameter to describe the coagulation process. As we are interested in the onset of coagulation, the peak temperature of the irradiated volume is of interest. However, this peak temperature cannot be measured directly, as the probing beam will always have a finite extent and penetration depth. However, conversion of the optoacoustically determined temperature to the peak temperature at the center of the irradiated area can be done via a time dependent conversion function<sup>9</sup>

$$f(t) = \frac{T_{\text{peak}}(t)}{T_{\text{mean}}(t)}, \quad (7)$$

which can be obtained mathematically. If we assume the calculated mean weighted temperature  $T_{\text{mean}}$  corresponds to the the optoacoustically determined temperature  $T_{\text{OA}}$  then the temperature of interest  $T_{\text{peak}}$  is given by:

$$T_{\text{peak}}(t) = T_{\text{OA}}(t) \cdot f(t). \quad (8)$$

## 2.3 Numerical Model

### Heat transfer and conversion function

We use COMSOL Multiphysics®, a commercially available finite element simulation software for modelling physics-based systems which allows coupling of several physical processes to evaluate the conversion function.

Our model for the temperature evolution during the treatment is a two-dimensional layer representation of the fundus consisting of the retina, the RPE and the choroid (see fig.1). The tissue parameters were assumed to be that of water ( $\rho = 993 \text{ kg/m}^3$ ,  $C_p = 4179 \text{ J/(kg K)}$ ,  $\kappa = 0.6 \text{ W/(m K)}$ ) and the absorption coefficients are chosen to be  $\mu_a = 1204 \text{ cm}^{-1}$  for the retina and  $\mu_a = 270 \text{ cm}^{-1}$  for the choroid and 0 everywhere else. The laser radiation is not simulated directly, as it is on a vastly different timescale than the heat conduction, instead we model the thermal effect of the light beam on the irradiated tissue. The RPE and the choroid are therefore treated as thermal heat sources according to

$$Q = \mu_a \cdot \phi(r) \cdot I_0 \cdot e^{-\mu_a z} \cdot \Theta(t), \quad (9)$$

where  $\phi(r)$  is the spatial laser light distribution, which in our case is a top-hat irradiation profile,  $I_0$  is the incident laser light intensity on the surface of the RPE, which decays exponentially with the penetration depth and  $\Theta(t)$  is the temporal laser light distribution

$$\phi(r) = \begin{cases} 1, & r < R \\ 0, & \text{else} \end{cases} \quad (10)$$

and

$$\Theta(t) = \begin{cases} 1, & t < \tau \\ 0, & \text{else} \end{cases} \quad (11)$$

The COMSOL module “Heat transfer” was used to solve eq. 4. As the problem is rotationally symmetric, the model is solved in a 2D geometry. After running the simulation, the spatially and temporally varying temperature profile is obtained (compare to Figure 2). From this temperature profile data set the maximum temperature can be extracted for every time  $t$ . Additionally, the optoacoustically determined temperature  $T_{OA}$  can be obtained by performing a surface integration according to eqs. 5 and 6.

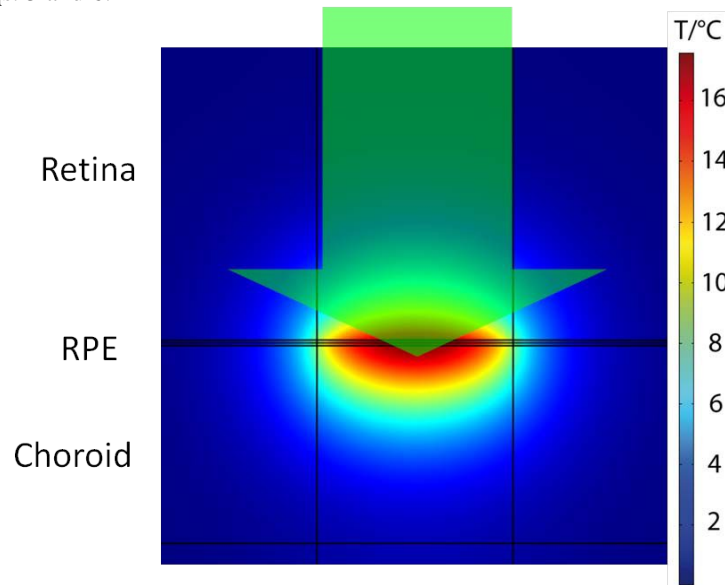


Figure 2 Temperature profile on the eyeground for  $t=200$  ms and an irradiation with  $P=10$  mW,  $\tau=200$  ms,  $d=100$   $\mu\text{m}$

Figure 3 shows the time progression of  $T_{\text{peak}}$  and  $T_{OA}$  over the course of an irradiation. Dividing the two curves yields the conversion function  $f(t)$  for the chosen parameters.

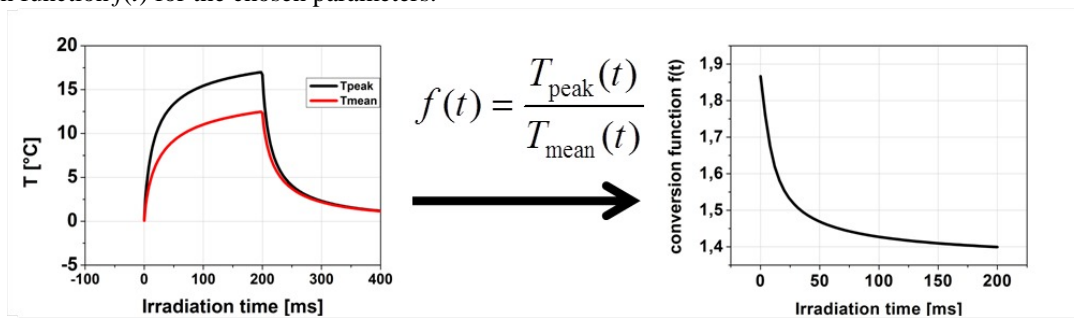


Figure 3 Time dependent temperature course for the mean and peak temperature during an irradiation with  $P=10$  mW,  $\tau=200$  ms,  $d=100$   $\mu\text{m}$  (left); time dependent conversion function for these irradiation parameters (right)

### Thermal expansion and pressure propagation

In order to model the pressure wave creation and propagation, the heat transfer model was extended and coupled with the solid mechanics module that solves structure-dynamic processes, such as thermal expansion and the propagation of pressure waves. The governing equations here are

$$\rho \frac{\partial^2 \mathbf{u}}{\partial t^2} - \nabla \cdot \boldsymbol{\sigma} = \mathbf{F} + \mathbf{v} \quad (12)$$

$$\boldsymbol{\sigma} - \mathbf{s}_0 = \mathbf{C} : (\boldsymbol{\varepsilon} - \alpha(T - T_{\text{ref}}) - \boldsymbol{\varepsilon}_0) \quad (13)$$

$$\boldsymbol{\varepsilon} = \frac{1}{2} [(\nabla \mathbf{u})^T + \nabla \mathbf{u}], \quad (14)$$

where  $\mathbf{u}$  is the displacement matrix,  $\boldsymbol{\sigma}$  the stress tensor,  $\mathbf{F}$  the pressure load,  $\mathbf{v}$  the velocity,  $\boldsymbol{\varepsilon}$  the strain tensor,  $\mathbf{s}_0$  and  $\boldsymbol{\varepsilon}_0$  are initial stresses and strains and  $\alpha$  is the thermal expansion tensor.

The absorbing central layer is irradiated with a short laser pulse (pulse duration 75 ns) with a pulse energy of 3  $\mu\text{J}$  (see Figure 4). The heating of the medium leads to a thermal expansion and a temporal increase in pressure that propagates as an ultrasonic wave. The wave passes an observer located 100  $\mu\text{m}$  above the RPE at the optical axis ( $r=0$ ), which allows us to investigate the excited pressure waves in the near field.

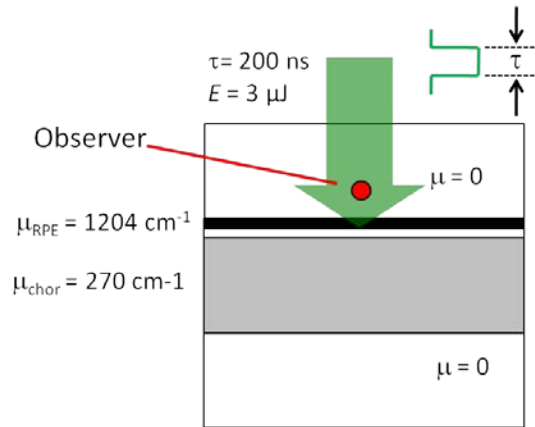


Figure 4 Schematic geometry for the optoacoustic pressure generation and propagation. A rectangular pulse with the pulse duration  $\tau$  and the Energy  $E$  is absorbed in the RPE and the choroid and due to the thermal expansion of the tissue an ultrasonic wave is generated. The wave propagates through the tissue and passes the observer that is located above the RPE.

The acoustic energy  $E_{\text{ac}}$  of a spherical wave with the temporal pressure distribution  $p(t)$  is given by<sup>10,11</sup> as

$$E_{\text{ac}} = \frac{4\pi r^2}{\rho \cdot c} \int p(t)^2 dt, \quad (15)$$

where  $r$  is the distance from the emission center to the observer.

Figure 5 shows the normalized pressure amplitude after propagating 2.5 cm through water as a function of the frequency, which is the distance from the retina to the cornea, where the optoacoustic transients can be detected. According to<sup>12</sup> the normalized pressure  $p/p_0$  as a function of the propagation distance  $x$  is given by

$$\frac{p(x)}{p_0} = e^{-\alpha(f)x}, \quad (16)$$

where  $p_0$  is the initial pressure value and  $\alpha(f)$  is the spectral absorption coefficient  $\alpha(f) = f^2 * 24 * 10^{-15} \text{ s}^2/\text{m}^2$ . The frequencies below 10 MHz propagate almost undisturbed, whereas frequencies above this threshold will be attenuated.

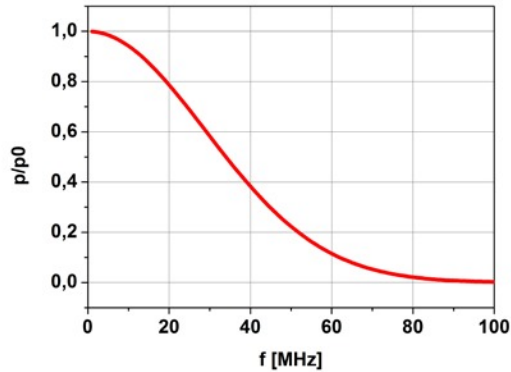


Figure 5 Transmission of ultrasonic waves of different frequencies after propagating 2.5 cm through water

The effect of the frequency dependent attenuation on the acoustic energy can be determined by performing a Fourier transform on the temporal pressure profile and then multiplying this with the characteristic attenuation function. An inverse Fourier transform yields the attenuated temporal pressure profile. By integrating the attenuated and unattenuated pressure profiles according to eq. 15, the effect of the attenuation can be quantified.

### 3. RESULTS

During atreatment, the conditions will not be as homogeneous as assumed with the calculations and parameters such as the absorption coefficients will vary from one irradiated volume to another. It is therefore imperative to assess the influence of the variation of the parameters that have a significant impact on the spatial and temporal behavior of the temperature profile. For that reason parametric sweeps of a number of these parameters have been performed. The rest were left constant in order to estimate the accuracy of our temperature determination when using a mathematically obtained function to calculate the peak temperature.

#### 3.1 Influence of the irradiation diameter on the conversion function

One crucial parameter to influence the temperature profile is the diameter of the incident laser light. The diameter was therefore varied from 50  $\mu\text{m}$  to 500  $\mu\text{m}$  in separate simulations. The conversion function was determined for each parametric step as described in 2.3. The result can be seen in Figure 6. There is a noticeable dependency of the conversion function on the irradiation diameter. The larger the diameter is, the lower the conversion function.

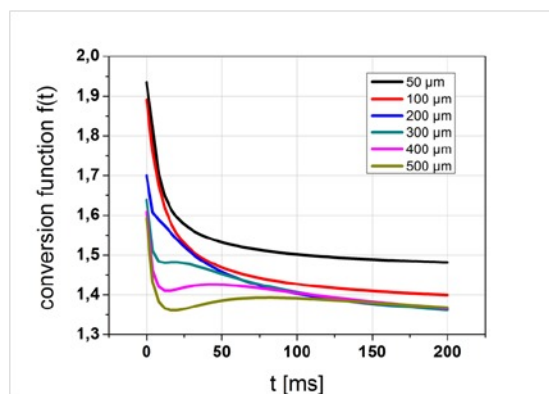


Figure 6: Conversion function for different irradiation diameters. The curves show a strong dependency on the diameter.

#### 3.2 Influence of the absorption coefficient on the conversion function

Another important aspect is the influence of the absorption on the temperature profile. A parametric sweep was performed, varying the absorption coefficient of the RPE by up to a factor of 2 from its literature value  $\mu_{a, RPE}$ , but

leaving the absorption coefficient of the choroid constant. This was done using an additional parameter  $a$ , which describes the sweep step absorption coefficient,  $\mu_{RPE,step}$  so that  $\mu_{RPE,step} = a * \mu_{a,RPE}$ . The irradiation power was  $P=100$  mW, the diameter was  $d=100 \mu\text{m}$ . The results can be seen in Figure 7.

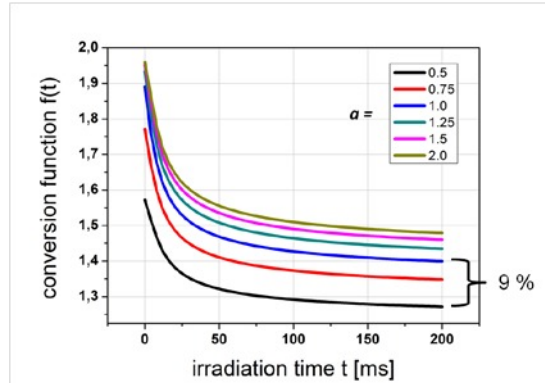


Figure 7 Conversion function for different irradiation absorption coefficients of the RPE. The curves show a strong dependency on the absorption coefficient.

Again, the curves show a dependency on a change of the absorption coefficient. For low RPE absorption coefficients, for example for  $a=0.5$ , i.e. the absorption coefficient is only half of its literature value  $\mu_{RPE,step} = a * \mu_a = 0.5 * 1204 \text{cm}^{-1} = 562 \text{cm}^{-1}$ , the values of the conversion function is about 9% smaller compared to the base curve at  $a=1$ .

In a second parametric sweep, the absorption coefficients of both the RPE and the choroid were changed simultaneously by up to a factor of 2, leaving the ratio constant. The results can be seen in Figure 8. There is only a small dependency on this simultaneous change in absorption coefficient of the RPE and the choroid.

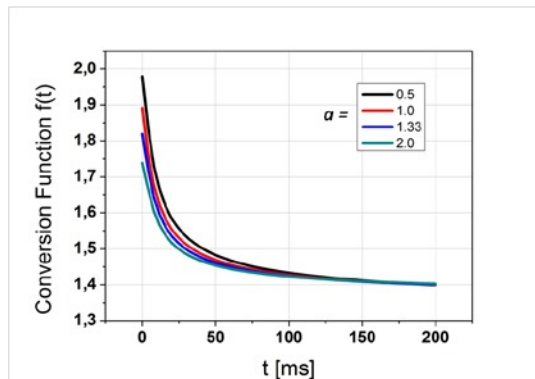


Figure 8 Conversion function for different irradiation absorption coefficients of the RPE and the choroid, when the ratio of the two remains constant. The curves show only a slight dependency on the absorption coefficient.

### 3.3 Frequency spectrum of photoacoustically excited pressure waves

The combined heat transfer and pressure propagation model was used to determine the influence of the irradiation duration on the excited frequencies during the ultrasonic pressure wave propagation. The pressure waves have to traverse the vitreous body before reaching the cornea, where they can be detected via an ultrasonic transducer. The model allows us to investigate a possible frequency dependent attenuation of the ultrasonic wave. Higher frequencies will be attenuated more strongly in water, and as the excitation durations in the experiments is 75 ns, modeling the process allows examining if there is a significant attenuation. The pulse duration of 75 ns was chosen and the modeled pressure waves were investigated regarding their frequency spectra by performing a Fourier transform on the pressure waves. The results can be seen in Figure 9. The calculated pressure profile (a) of the transient wave was fourier transformed and multiplied with the characteristic transmittance curve for water (c) for a propagation distance of 25 mm, corresponding to the eye length. The resulting frequency distribution is inverse fourier transformed to yield the attenuated pressure curve

(d). By squaring the pressure curves, the ratio of the acoustic energies can be determined as  $E_{ac,atten}/E_{ac,unatten} = 0.24$  by integrating the pressure profiles as seen in (e).

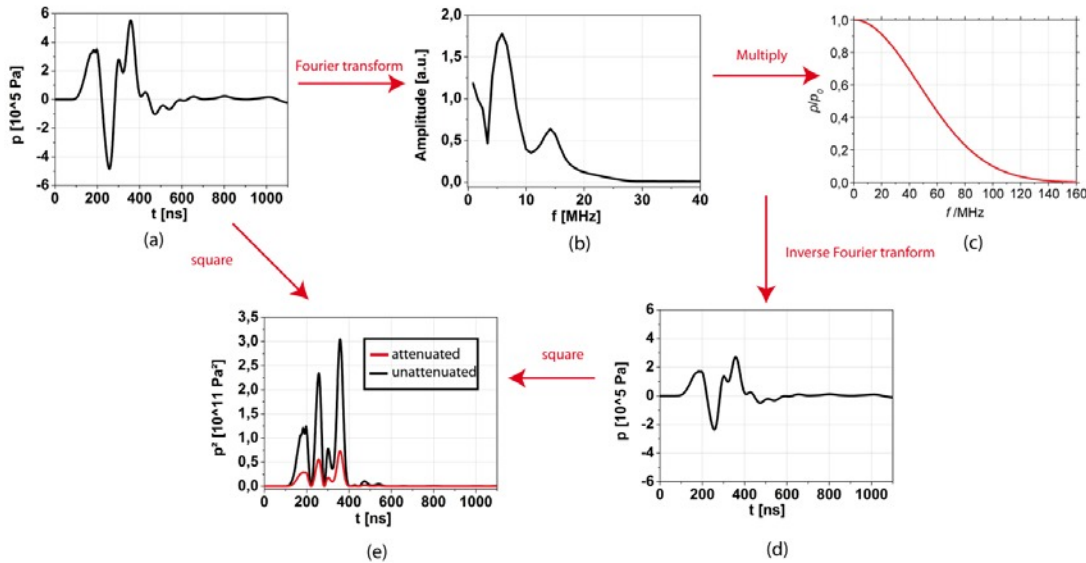


Figure 9 Calculation of the attenuated energy fraction from the simulated pressure profile at the observer (a). The Fourier transform yields the spectral distribution (b). By multiplying the spectral distribution with the characteristic transmittance curve for a propagation distance of 2.5 cm (c) and subsequent inverse Fourier transformation the frequency dependent attenuation of the pressure profile is gained (d). By squaring the attenuated and unattenuated pressure profiles the acoustic energy of both pressure waves can be determined according to eq. 15.

## 4. DISCUSSION

### 4.1 Conversion function

It has been shown that the temperature conversion function, and therefore the accuracy of the peak temperature determination is dependent on the irradiation diameter as well as the change in absorption coefficient in one absorbing layer, but shows little variation, if the absorption coefficients of both layers are changed homogeneously. In the former case, the higher the absorption coefficient is, the higher the conversion function becomes, as it leads to more absorption at the RPE and therefore a lower temperature in the choroid, which lowers the value of the temperature. In the latter case, the remaining small discrepancy can be attributed to some of the light not being absorbed, for example for  $a=0.5$ . If the absorption coefficients in the RPE and the choroid is e.g. only at half their literature value, about 7% of the incident light escapes from the geometry. This leads to a discrepancy in the conversion function of about 2.5%.

The change in irradiation diameter can be accounted for, it is known ahead of the treatment. However, other effects that influence the irradiation diameter, such as beam defocusing or scattering, which reduce the accuracy of the measured temperature are not taken into account here. The influence of these effects on the beam diameter is currently under investigation.

On the other hand, the variation of the absorption coefficient is not known prior to the treatment and will therefore introduce uncertainties in the measured temperature. It is however reasonable to assume that the density of the absorbing melanosomes in the RPE and the choroid is linked, so that the situation as shown in Figure 8 seems more likely than that in Figure 7. There will be variations of the absorption coefficients though and this will reduce the accuracy of the peak temperature determination. The error as determined in our investigation is therefore estimated to be between 2.5% and 9%.

### 4.2 Frequency dependent attenuation of propagating pressure waves

It has been shown, that there is a significant frequency dependent attenuation of 76% over a distance of 25 mm of the pressure wave when the ultrasonic waves are excited with a pulse duration of 75 ns. However, the used equations are derived for the acoustic far field and a point source. We do not fully meet these criteria, however, this should serve as a

rough estimation of the influence of the attenuation in water. For shorter pulse durations the influence of the acoustic attenuation becomes larger, however the condition of the stress confinement is not met for longer pulse durations, which in turn decreases the pressure amplitude and makes detection more difficult.

### 4.3 Model limitations

There are a couple of limitations to the model. First, we cannot incorporate scattering into the model in a direct way. The timescale and the dimensions of the light propagation differ too much from the processes of heat conduction and pressure propagation and would make the simulation too time- and memory consuming. Scattering could however indirectly be approximated by introducing another attenuation parameter or in the case of forward-scattering an increase in irradiation diameter during the propagation through the eye.

Secondly, the heat diffusion model does not necessarily describe the measured temperature directly. As we infer the temperature from a pressure measurement, the resulting temperature is dependent on the pressure-temperature calibration<sup>9</sup>. However, the correlation between pressure and temperature is nonlinear. Therefore the influence of the detected pressure wave on the temperature determination has to be taken into consideration.

## 5. CONCLUSION

In this work a numerical model using COMSOL Multiphysics ® has been implemented to determine the physically relevant peak temperature from the mean weighted volume temperature as it is measured with optoacoustics during retinal photocoagulation. Several parametric sweeps have been performed to test the limits of this conversion within relevant constraints. The results indicate an uncertainty in the determination of the peak temperature between 2.5 and 9 % if the unknown individual absorption coefficients of the RPE and choroid change by a factor of 2. An influence of the beam diameter was found, resulting in the need of a finite set of conversion functions for the different irradiation diameters.

Furthermore it was shown, that there is considerable frequency dependent sound attenuation when exciting the pressure waves with a pulse duration of 75 ns. Further work should examine the pressure waves in the far field and the most suitable pulse duration and according detector frequency bandwidth in order to maximise the pressure excitation and to optimize the electrical signal conversion.

## REFERENCES

- [1] Early Treatment Diabetic Retinopathy Study Research Group. "Early photocoagulation for diabetic retinopathy. ETDRS report number 9" *Ophthalmology* ;98(5 Suppl):766–85 (1991)
- [2] Early Treatment Diabetic Retinopathy Study Research Group, "Photocoagulation for diabetic macular edema. Early treatment diabetic Retinopathy Study Report No. 1," *Arch. Ophthalmol* 103( ), 1796-1806 (1985)
- [3] Macular Photocoagulation Study Group, "Treatment techniques and clinical guidelines for photocoagulation of diabetic macula edema: Early Treatment Diabetic Retinopathy Study Report Number 2", *Ophthalmology*, 94(7), 761-774 (1987)
- [4] Manohar, S., Kharine, A., van Hespren, J. C. G., Steenbergenm, W., and van Leeuwen, T. G., "The Twente Photoacoustic Mammoscope: system overview and performance", *Phys. Med. Biol.* 50, 2543–2005)
- [5] Xu, M. H. and Wang, L. V., "Photoacoustic imaging in biomedicine", *Rev.Sci. Instrum.* 77, 041101 (2006)
- [6] Esenaliev, R. O., Larina, I. V., Larin, K. V., and Motamedi, M., "Realtime optoacoustic monitoring during thermotherapy", *Proc. SPIE* 3916, 302–310 (2000)
- [7] Kandulla, J., Elsner, H., Birngruber, R., and Brinkmann, R., "Noninvasive optoacoustic online retinal temperature determination during continuous-wave laser irradiation", *J Biomed Opt* 11, pp. 041111 (2006)
- [8] Brinkmann, R., Koinzer, S., Schlott, K., Ptaszynski, L., Bever, M., Baade, A., Luft, S., Miura, Y., Roider, J., Birngruber, R" Real-time Temperature Determination during Retinal Photocoagulation on Patients", *J Biomed Opt*, 17(6), 061219 (2012)
- [9] Schlott, K., Koinzer, S., Ptaszynski, L., Bever, M., Baade, A., Roider, J., Birngruber, R., Brinkmann, R." Automatic temperature controlled retinal photocoagulation", *J Biomed Opt*, 17(6), 061219 (2012)
- [10] Cole, R. H., "underwater Explosions", Princeton U.P., Princeton, 1948.
- [11] Vogel, A., Lauterborn, W., Acoustic transient generation by laser-produced cavitation bubbles near solid boundaries", *J. Acoust. Soc. Am.* 84(2), (1988)
- [12] Kuttruff, H., "Physik und Technik des Ultraschalls", p. 415, Hirzel: Stuttgart, (1988)